Using High-Resolution Digital Photography and Micro-CT Scanning to Investigate Deathwatch Beetle Damage to an Historic Timber from HMS *Victory*

Fiona Brock, Richard Southwell, Zoë Hazell, Roland Wessling, Matthew Green & Diana Davis

Published online: 16 Jan 2022.

Submit your article to this journal ⬈

Article views: 33

View related articles ⬈

View Crossmark data ⬈

Association for Environmental Archaeology

Routledge
Taylor & Francis Group

Using High-Resolution Digital Photography and Micro-CT Scanning to Investigate Deathwatch Beetle Damage to an Historic Timber from HMS *Victory*

Fiona Brock [a], Richard Southwell[a], Zoë Hazell[b], Roland Wessling[a], Matthew Green[c] and Diana Davis[d]

[a]Cranfield Forensic Institute, Cranfield University, Defence Academy of the United Kingdom, Shrivenham, UK; [b]Historic England, Portsmouth, UK; [c]Rentokil-Initial PLC Science, Technology & Special Projects Team, Crawley, UK; [d]National Museum of the Royal Navy, Portsmouth, UK

ABSTRACT

Wood-boring insects such as the deathwatch beetle can cause significant damage to historical artefacts and timbers, but the extent of internal damage (and tunnelling activity in general) can be difficult to understand and quantify without the use of destructive sampling techniques. This study explored the potential of high-resolution photography and micro-computed tomography (micro-CT) to investigate beetle activity and inform on the extent of internal damage to a timber from HMS *Victory*. Micro-CT imaging has allowed the visualisation of deathwatch beetle activity within the timber, revealing differences in tunnelling behaviour preferences for adult and larval forms. Digital techniques were developed to determine the surface area of flight holes on some wooden blocks but were less successful for those blocks where the external surfaces were darkened with age. It was not possible to accurately determine the internal volumes of beetle tunnels within blocks of timber due to the presence of frass, which was found to be virtually indistinguishable digitally from the wood matrix.

Introduction

HMS *Victory* is an English Royal Navy first-rate 'ship of the line' warship that continues to be in commission since her launch in May 1765. Although seeing high profile service in the American War of Independence, the French Revolutionary War and the Napoleonic War, she is probably best known as the flagship of Vice-Admiral Nelson in the Battle of Trafalgar (1805). It was during this battle that she was greatly damaged, subsequently undergoing a series of repairs and refits, and her active career finally ended in 1812. In 1814, the ship was dry-docked and underwent a major refit, and much of what is seen today dates to this period of repair. After being accidentally rammed in Portsmouth Harbour in 1903, a comprehensive restoration programme began, leading to her permanent dry-docking at Portsmouth in 1922, when *Victory* was moved into the dockyard's No. 1 Basin. Work included reverting major structural changes and redesigns that had been carried out in the 1800s (see McGowan 1999). *Victory* remains in dry dock there today, in the care of the National Museum of the Royal Navy (NMRN), as the flagship of the First Sea Lord.

Victory has suffered particularly from damage by the wood-boring deathwatch beetle, *Xestobium rufovillosum* (Coleoptera: Anobiidae). They are found throughout Europe (native to the British Isles) and attack hardwood (angiosperm) trees, most commonly oak and willow (Hickin and Edwards 1975). They will readily attack sound sapwood but only attack heartwood that has been modified by fungal decay (McCaig and Ridout 2012, 147–148; Hickin and Edwards 1975, 123–125). Their damage consists of a series of tunnels (galleries) within the wood, which contain the frass waste – a mix of bore dust and their characteristic bun-shaped excreted pellets. External evidence of damage includes their circular exit (flight) holes (3–6 mm in diameter; McCaig and Ridout 2012), which are formed when the adult beetle emerges from the wood. Although this is reported to occur in late April/early May, they are seen to emerge on *Victory* almost all year round (with smaller numbers in winter) (Davis 2018). The beetles are able to thrive on the ship due to problems with high relative humidity (often recorded above 70%) and the difficulties in controlling the same, since the ship is exposed to the exterior conditions and is poorly sealed. Freshwater ingress at various points can cause localised saturation of the timbers, resulting in moisture contents in excess of 20%, leading to fungal growth and decay (Davis, 2020).

Given that the main timber used in ship construction was oak and that ships are constantly exposed

CONTACT Fiona Brock ✉ f.brock@cranfield.ac.uk 🖃 Cranfield Forensic Institute, Cranfield University, Defence Academy of the United Kingdom, Shrivenham, SN6 8LA, UK

to damp environmental conditions, it is not surprising that *Victory* was susceptible to attack by *X. rufovillosum*. It was first discovered in 1932 (Bugler 1966, 87), and over the period during which annual counts were made (1937 until 1988, excepting a few years; see both Bugler (1966) and McGowan (1999, 100)), numbers peaked in 1947 at 16,034 individuals (Bugler 1966, 90). Managing the infestation has in the past included removing the decaying and susceptible oak timbers and replacing them with teak and iroko (both more-resistant tropical hardwoods), supplemented with the use of insecticides (as spray applications and/or fumigations). It is anticipated, however, that in upcoming programmed works, oak will be the primary timber used to repair the ship, remaining true to the original build. This poses a conservation challenge in managing the beetle and keeping the new timber free from infestation.

Any internal damage to wood will affect the strength and loading capabilities of the timber, which in turn will have implications for structural safety. For smaller wooden artefacts, beetle infestation can result in damage to, and potentially the total loss of, unique archaeological and historical objects. The development and application of non-destructive techniques to investigate and, where possible, quantify, the extent of internal damage to timbers caused by beetles, is therefore important to those curating and protecting wood-based cultural heritage. Such studies include Ungurean (2012), for example, who characterises the damage caused by a range of different anobid beetles to historical wooden timbers outside, while Hedges (2012) assesses flight hole damage in historical printing wood blocks to quantify the internal damage caused by two different species of beetle.

Methods for determining marine-borer damage to internal wood structures include 2D X-radiography, which has been routinely used to investigate damage and presence of marine borers within wooden remains and is particularly useful where remnants of the calcareous linings are visible in the case of shipworm (*Teredo navalis*) (e.g. Knight, Cousins, and Parham 2019). For samples where damage is much smaller-scale and where no distinctive physical remains are left, an alternative is X-ray micro-computed tomography (micro-CT) (see Steppe et al. 2004; Van den Bulcke et al. 2009; Brodersen 2013). The technique has been used to trace the tunnels of wood-boring larvae (xiphydriid woodwasps; Jennings and Austin 2011) and study the respiratory development of wood-boring beetle larvae (Lehmann et al. 2021).

Micro-CT is a non-invasive technique whereby a series of 2D X-radiographs of an object are taken while it is mounted on a stage and rotates through 360°. These X-radiographs are digitally reconstructed to produce a 3D visualisation of the internal structure of the object in any plane. The technique has been shown to produce wood anatomical features equivalent to those observed with classical optical microscopy of stained thin sections, without requiring labour-intensive and costly preparation of samples (Steppe et al. 2004). However, the spatial resolution of the image data generated depends on a variety of factors, and while it can typically be on the micron or, in some instances, sub-micron scale, this requires sectioning of small blocks or thin sections (e.g. Steppe et al. 2004; Van den Bulcke et al. 2009), which is not appropriate for many historical or archaeological specimens.

Micro-CT imaging of wood has been used successfully for identifying wood types and recording other dendrological features, including those on archaeological artefacts of different preservation conditions e.g. desiccated wood (Whitau et al. 2016) and mineralised wood (Stelzner and Million 2015; Haneca et al. 2012), and on non-archaeological remains e.g. wood within soil blocks (Stelzner and Million 2015). It has also been used to provide 3D internal visualisation of the extent of damage to wood by fungal attack (e.g. Van den Bulcke et al. 2008; McGovern et al. 2010).

As well as visualising wood structure, the data can be processed to provide further quantitative information, for example, measuring the diameter, transverse cross-sectional surface areas, vessel density and porosity of wood (Steppe et al. 2004); porosity, pore-size, and pore-connectivity of wood charcoal (Bird et al. 2008); and the length and volume of marine bivalve tunnels in submerged wood (Amon et al. 2015; Eriksen et al. 2016). For these and similar studies, bespoke software is often developed for the specific sample material and object(s) of interest. In most cases, these utilise a method called 'segmentation', whereby the digital image is partitioned into 'segments' of similar voxel grey value or density, setting threshold values to define the boundaries between materials such as empty wood vessels (lower grey value) and the surrounding wood matrix (higher grey value).

This study aimed to explore the potential of micro-CT scanning to investigate the patterns and extent of internal damage to dry timbers caused by prior infestation by deathwatch beetle and to develop image analysis protocols for quantifying this damage. Specific research questions addressed by studying a timber from *Victory* were:

- Can tunnelling preferences of the insects be identified? If so, what are they? (For example: axial versus radial alignments, earlywood versus latewood, fibre cells versus wide multiseriate rays, lines of weakness, e.g. cracks).
- Is it possible to quantify the internal damage to timbers, i.e. to determine the volume of wood missing due to insect galleries?
- Is surface damage indicative of the degree of internal damage?

To investigate this third question, high-resolution digital photographs were taken of the flight holes on the outer surface(s) of the timbers, with the aim of developing a digital method to determine the area of the flight holes. If surface damage was found to be indicative of the extent of internal damage, analysis of high-resolution digital images of archaeological artefacts or *in situ* historic timbers showing signs of infestation could potentially reduce the need for sub-sampling or complete removal of such timbers by conservators and archaeologists concerned by insect damage.

Methods

Sample Selection and Description

A single timber of *Quercus* sp. (oak) from *Victory* was used for this study (Figure 1); it had been removed from the ship's hull between 1955 and 2000 during routine, on-going restoration work, because it showed evidence of damage by *X. rufovillosum*. There is no secure record of its original *in situ* position or orientation, although it is thought to be from a futtock (part of one of the ship's 'rib' frames), thereby dating to between 1759 and 1816. Since its removal, it has been kept in storage at the Royal Navy dockyard, then by a private owner, and since 2012 by the NMRN. It is most likely to be heartwood, as sapwood tended to be (though not always) removed by shipwrights during conversion, but this was not checked prior to the destructive analysis of the blocks following this study. The smooth, even faces are inferred to be original outer edges of the timber, with the darker colour resulting from factors associated with ageing and/or exposure. It is not thought to have been topically treated, as futtocks are located within the double skin of a ship's structural frame. This timber was selected as it did not contain any high-density materials (such as copper nails or lead-painted surfaces) that would have affected the imaging.

Quercus has a very distinctive wood structure. Its main (macroscopic) characteristic features are that it: (i) is 'ring porous' (i.e. large vessels are concentrated in the earlywood growth of each annual ring), and (ii) has rays that are both uniseriate (one cell wide), and multiseriate (up to 30 cells wide) the latter of which can be 1 mm wide and 1–5 cm high (Schweingruber 1990). Recognising these features will help understand and interpret the insects' pattern of damage in the wood itself.

Sub-Sampling

The timber was cut into rectangular cuboid blocks using a band saw. The blocks had square end faces (approx. 40×40 mm), and were 60–120 mm long; the block lengths varied depending on how much wood volume was missing due to decay. The maximum length (120 mm) was the largest that could be imaged in a single micro-CT scan. Some blocks had to be discarded as they were so heavily degraded and/or fragile that they disintegrated on handling. A total of 15 blocks remained for imaging.

Not all the blocks were cut on the same alignments; of those described below, some (Blocks 1a, 1b) have

Figure 1. The investigated oak timber (previously removed from *Victory*) before subsampling. Note the original, darker and smoother, outer surface. *Image taken by R Southwell.*

the transverse section on the long axis of the block, and the remainder (Blocks 6a, 7a) have it on the short axis. Although this is not significant for the micro-CT data, which can be viewed in any plane, the small ends of the blocks were not photographed.

DSLR Photography

High-resolution sRGB (standard Red-Green-Blue) photographs were taken of the four largest faces of the 15 blocks but not of the blocks' ends. This was done in a white LED-lit diffused light box to avoid shadow, using a Canon EOS 450D DSLR (digital single-lens reflex) camera, with a Canon EF-S 18–55 mm f/3.5-5.6 IS STM lens. The settings used are given in Table 1. Each block was mounted in the same way to allow for comparison, and ensuring that no surfaces were photographed from an angle, which could have affected the analysis of the area of the flight holes. A mini photomacrographic scale (with measurements in millimetres) was used in each image to allow calibration for image processing.

Micro CT-Scanning

Micro-CT scanning was undertaken using a Nikon XT H225 scanner (Nikon Metrology, Tring, UK) with Perkin Elmer XRD 0820 flat panel detector and a tungsten reflectance target. Scans were run at an accelerating voltage of 110 kVp and a current of 42–45 μA, with an exposure time of 354 ms. The exposure time was deliberately set short due to time constraints for imaging all 15 blocks. The instrument was set to optimise the number of projections taken (typically 1400–1571) with two frames taken per projection. Each wood block was scanned at the same magnification, with the resultant voxel size for each sample of 137 μm.

Micro-CT data was reconstructed using CT Pro 3D software (Nikon Metrology, Tring, UK), and data visualised and processed using VG StudioMax v2.1 (Volume Graphics GmbH, Germany). Image stacks with an individual thickness of 200 μm were generated as TIFF files in all three planes (parallel to surfaces of the block) for subsequent analysis of tunnel volume (see below), as well as for the visual images presented here.

Table 1. Details of the DSLR camera and image settings used for recording the external surfaces of the wood blocks.

Camera settings	Image settings
Depth of field: f22	High-resolution JPEG
Exposure time: 1/5 sec	4272 × 2848 pixels
ISO speed: 100	Horizontal and vertical resolution: 72 dpi
Focal length: 49-58 mm	Bit depth: 24 bit
Flash: off	

Note: The focal lengths were adapted using a crop factor of 1.62 based on the camera's sensor size.

2D X-radiographs were also taken of two blocks (Blocks 1a and 1b) using the same settings as above (with a current of 50 μA), Inspect-X software (Nikon Metrology, Tring, UK) and recorded using a 64 frame average and the 'sharpen more' tool.

Image Analysis

Analysis of Surface Flight Holes Using DSLR images

The open-source software ImageJ – as distributed by FIJI (Schindelin et al. 2012) – was used for the image processing. Advantages of ImageJ for this study are that it supports JPEG file format (as used here for the RGB images), is capable of processing sequences of 100s–1000s of images, and has a selection of filtering options available.

Prior to any image manipulation and analysis, the DSLR images were first calibrated in mm (according to the number of pixels along the scale bar accompanying the image) and then converted to 8-bit grey-scale JPEG files. The images were then stack cropped to remove unwanted background image data.

To calculate the total area of beetle flight holes on the surface of the blocks (be they original outer, or more recently cut or broken, faces), the holes had to be digitally isolated from the wood matrix. A median filter was first applied to the images to apply a smoothing operation to de-emphasise the natural grain structure and cracks within the wood. A background subtraction operation was implemented to blend the timber with the surrounding background to leave the tunnels as the only remaining features. A threshold filter was then applied to distinguish between the beetle tunnels (the regions of interest, ROIs) and the rest of the image. Watershed segmentation was then applied to split the tunnels into smaller 'particles' for area measurement. Where necessary, any remaining undesirable features (e.g. cracks within the wood) could be excluded in the area measurement by setting minimum areas, specific pixel intensity, and/or the circularity of the feature. The total area of flight holes was calculated for each face of the block by summing the individual 'particle' areas.

Determination of the Total Volume of Wood Blocks

The total volume of each complete block was calculated by multiplying the measured length by the width by the depth. However, for the irregular-shaped blocks the surface area of the wood samples' cross-sections was calculated using MatLab (v. 2018b; 9.5.0.1178774). Before the analysis, all images were loaded into Pixelmator Pro (1.6.4; 200601.1136) and the *Highlights*, *Contrast* and *Black Point* settings
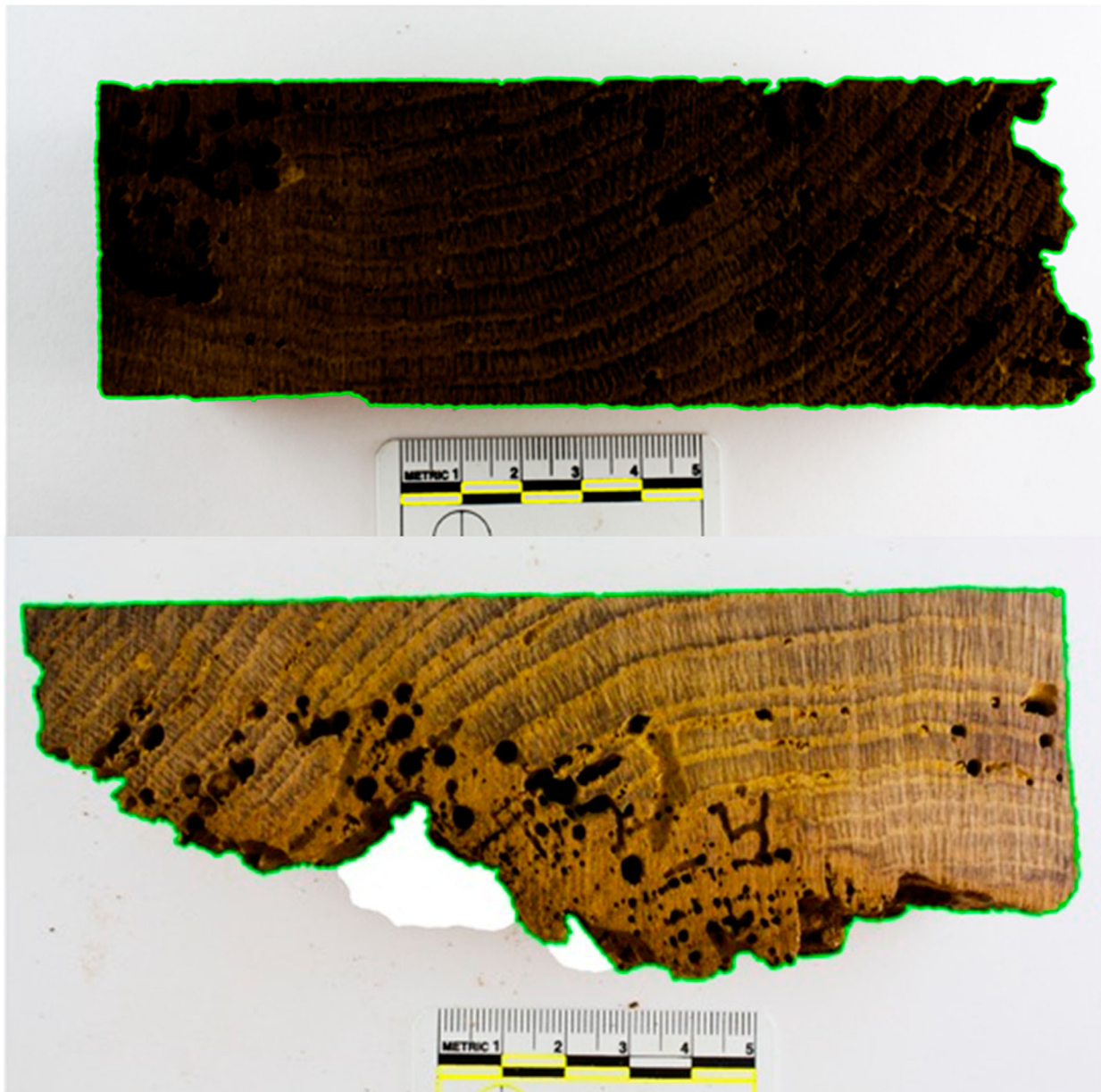
Figure 2. Matlab analysis of (a) Block 1a and (b) Block 3b to determine surface area. The yellow outlines show the automatically detected areas within the photographic scale (each 1 cm wide); the green outline shows the automatically detected border between foreground (sample) and background. Both outline types were superimposed onto the original image rather than the binary images from which they were derived.

increase to 100% to improve overall contrast between the sample and the background for automatic detection in MatLab. The MatLab function then performed two basic tasks. Firstly, it detected the photographic scale in the images (Figure 2) and measured its dimensions to later convert the area measurement of the sample from pixels to square centimetres. Using the histogram of each image, the function set a threshold between 0 and 255 and converted the image into a binary black-and-white image. In that image, it isolated shapes specific to the photographic scale (which are of known dimensions) and from this calculated a conversion factor. In the second step, the original image was again converted into a binary one but using a threshold that was specific to the colour range of the sample rather than the photographic

scale. All items in the image other than the actual sample were eliminated from the binary image so that only the sample remained (Figure 2) and its area measurement was determined using the *regionprops* function. For some samples (e.g. Figure 2(a)) the contrast was altered to enhance isolation of the sample from the background. However, despite the use of diffused lighting, the contrast between the foreground and background was not sufficient for completely automatic outline detection for some samples (e.g. Figure 2(b)) and the 'magnetic lasso' tool in Pixelmator Pro was used to manually improve the background.

The volume of the irregular blocks could then be calculated by multiplying the surface area by the thickness of the block.

Determination of Total Internal Tunnel Volume Using Micro-CT Images

The same approach that was used to calculate the area of surface flight holes from the DSLR images with ImageJ was applied to calculate the tunnel area on each of the micro-CT slices. The total volume of beetle tunnels per slice was calculated by multiplying the sum of the tunnel ('particle') areas by the slice thickness (200 μm). The total tunnel volume per sample block was then calculated as the sum of the volume from all slices.

The tunnel volume was calculated twice for each block using TIFF slices from two different planes to check for reproducibility.

This approach requires the assumption that the tunnels remain constant in depth and direction throughout each slice (although variations in both of these will naturally introduce some imprecision) but was used to ensure continuity with the method applied to the DSLR images for calculating surface tunnel area.

Determination of Total Internal Tunnel Volume Using VG StudioMax

For comparison, tunnel volume was also determined for two blocks (Blocks 6a, 6b) using VG StudioMax v2.1 software. The object was first aligned along the z-axis before a cuboid region of interest (ROI) was extracted for analysis from the total data volume. This was necessary to ensure that air surrounding the wooden block was not included within the total tunnel volume but resulted in small regions of the block being excluded from the calculations and was therefore not suitable for analysis of the irregular-shaped blocks.

Segmentation was then applied to isolate the empty tunnels from the wood according to the voxel grey-scale density using the isovalue mode for automatic surface determination. Empty tunnels had a low grey-scale value based on the density of air (appearing black on the micro-CT images) and were clearly distinct from the wood matrix, but the isosurface had to be set manually to best distinguish between the early wood and the frass that had very similar greyscale densities. The total volume of the low greyscale density segment (i.e. the empty tunnels) was then calculated from the object properties of the ROI.

Once the empty tunnels had been isolated by this process, the rest of the sample matrix could be extracted and the tunnel volume grey values 'inverted', allowing the individual tunnels to be visualised from any direction.

Results

Imaging of Blocks

Here, the imaging results for a selection of blocks are presented. The blocks have been chosen on the basis of the techniques used, the extent of internal damage, and the range of features and characteristics shown.

Blocks 1a and 1b

These two were the only blocks to have had initial exploratory 2D X-Radiographs taken. Block 1a (Figure 3) is a near-complete rectangular cuboid,
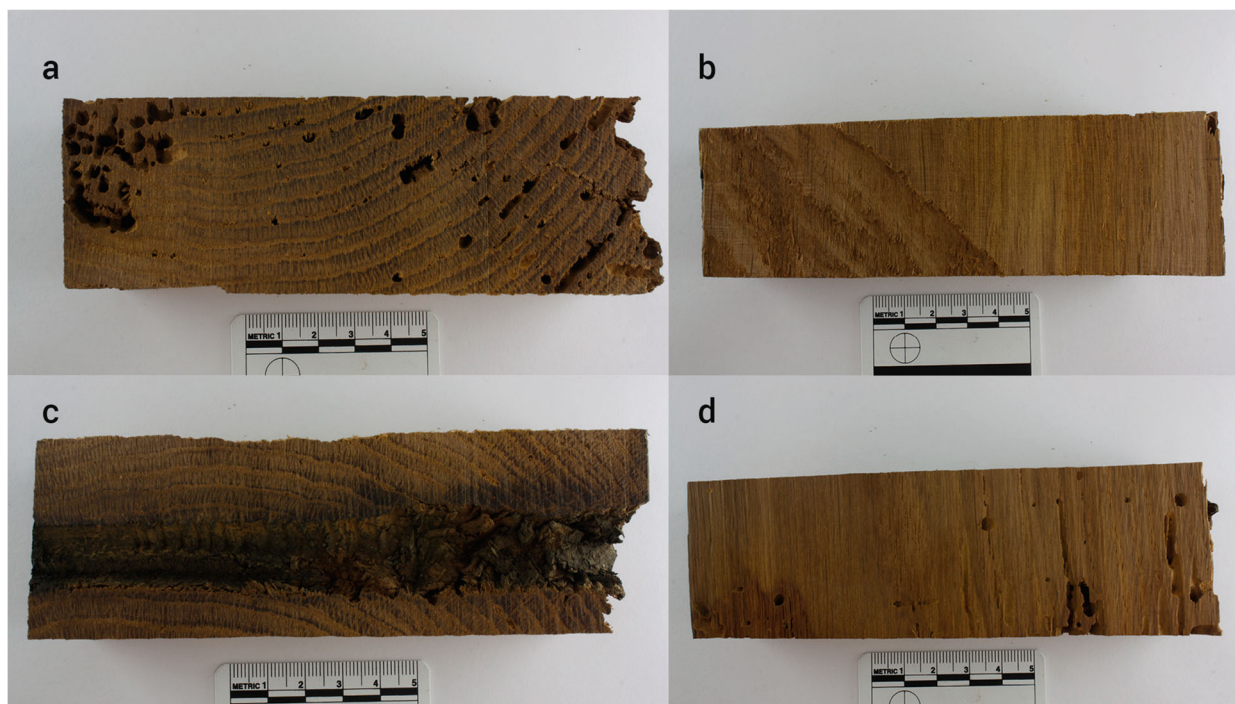

Figure 3. Block 1a, showing the reverse faces on the top and bottom rows.
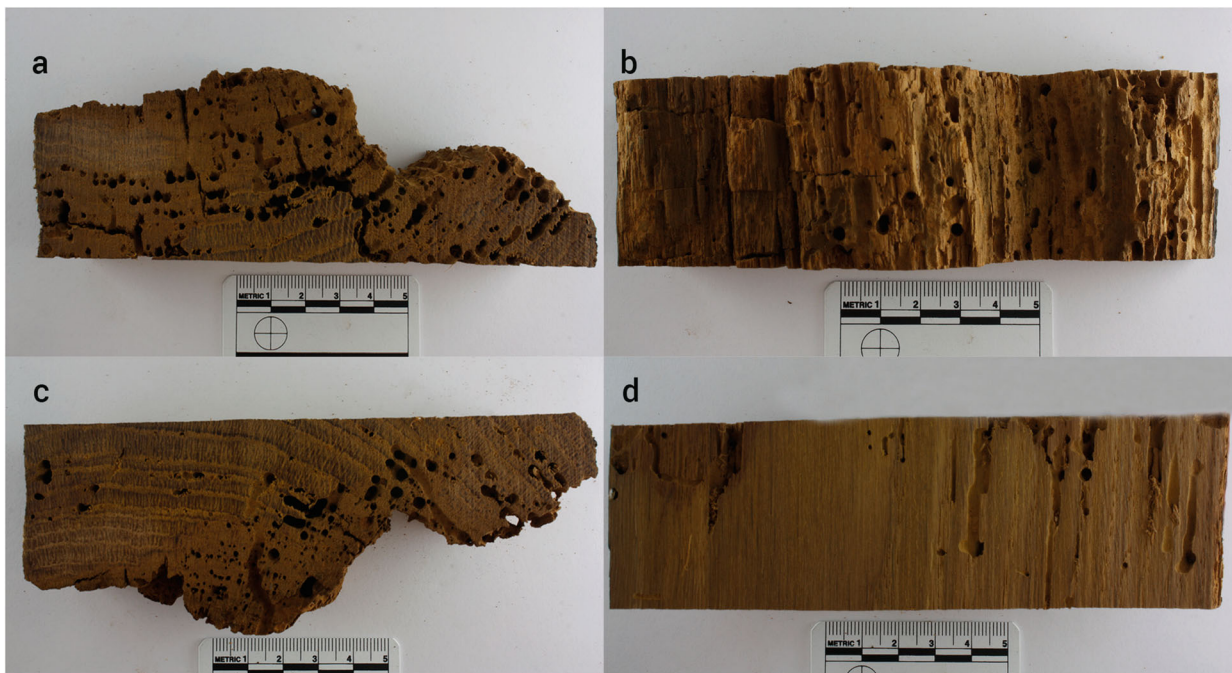
Figure 4. Block 1b, showing the reverse faces on the top and bottom rows.

with an uneven void running through the centre where a fastening (likely an oak treenail (dowel) or large copper spike) to hold the ship's timbers together would have been (Figure 3(c)), whereas Block 1b (Figure 4) is irregularly-shaped due to missing wood mass.

The X-radiographs of Blocks 1a and 1b are shown in Figure 5. Although they demonstrate the tunnels' presence and thereby some detail of the level of infestation, they represent the sum of X-ray absorption through the complete thickness of the sample and so cannot provide insights into the 3D nature of the tunnels.
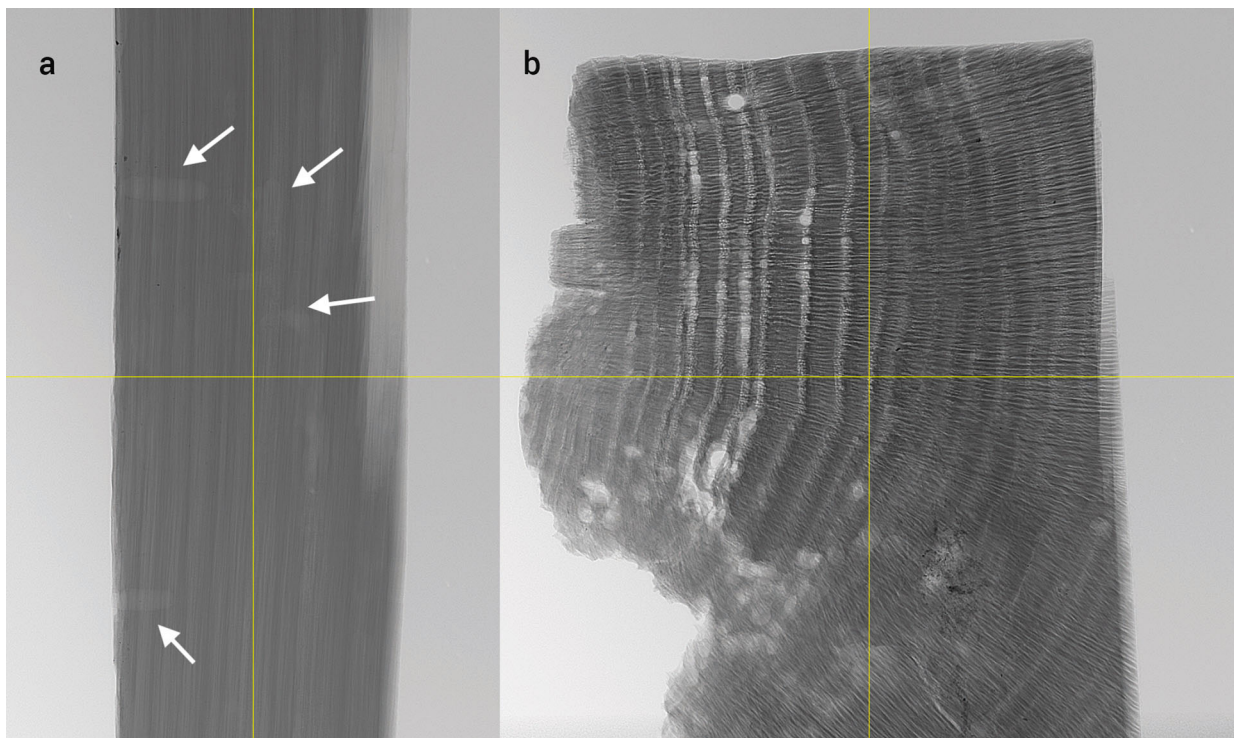

Figure 5. X-radiographs of Block 1a (a) and Block 1b (b). Note that for Block 1a, the direction of imaging is not completely perpendicular to the flat surface plane of the blocks but was optimised to visualise the tunnels which can be seen penetrating the wood from the left-hand side of the image (indicated by white arrows).

The X-radiograph showing the transverse section of the wood (Figure 5(b)) shows characteristics of the wood itself (i.e. the growth rings) as well as some insect damage manifest as tunnels, including holes of different diameters. An area of wood along some of the uneven, degraded edge of the fragment appears to be paler in appearance on the X-radiograph (i.e. with a lighter greyscale value) than the rest of the sample. Close inspection of the wood block itself (Figure 6(a)) appears to show the same area being slightly darker in colour than the rest of the sample and to have lost some of its structural definition. The same region of wood also appears to have a slightly darker greyscale value than the rest of the wood on the corresponding micro-CT slices (Figure 6(b,c)). This difference in appearance within Block 1b could be due to some other form of degradation (see below for further discussion).

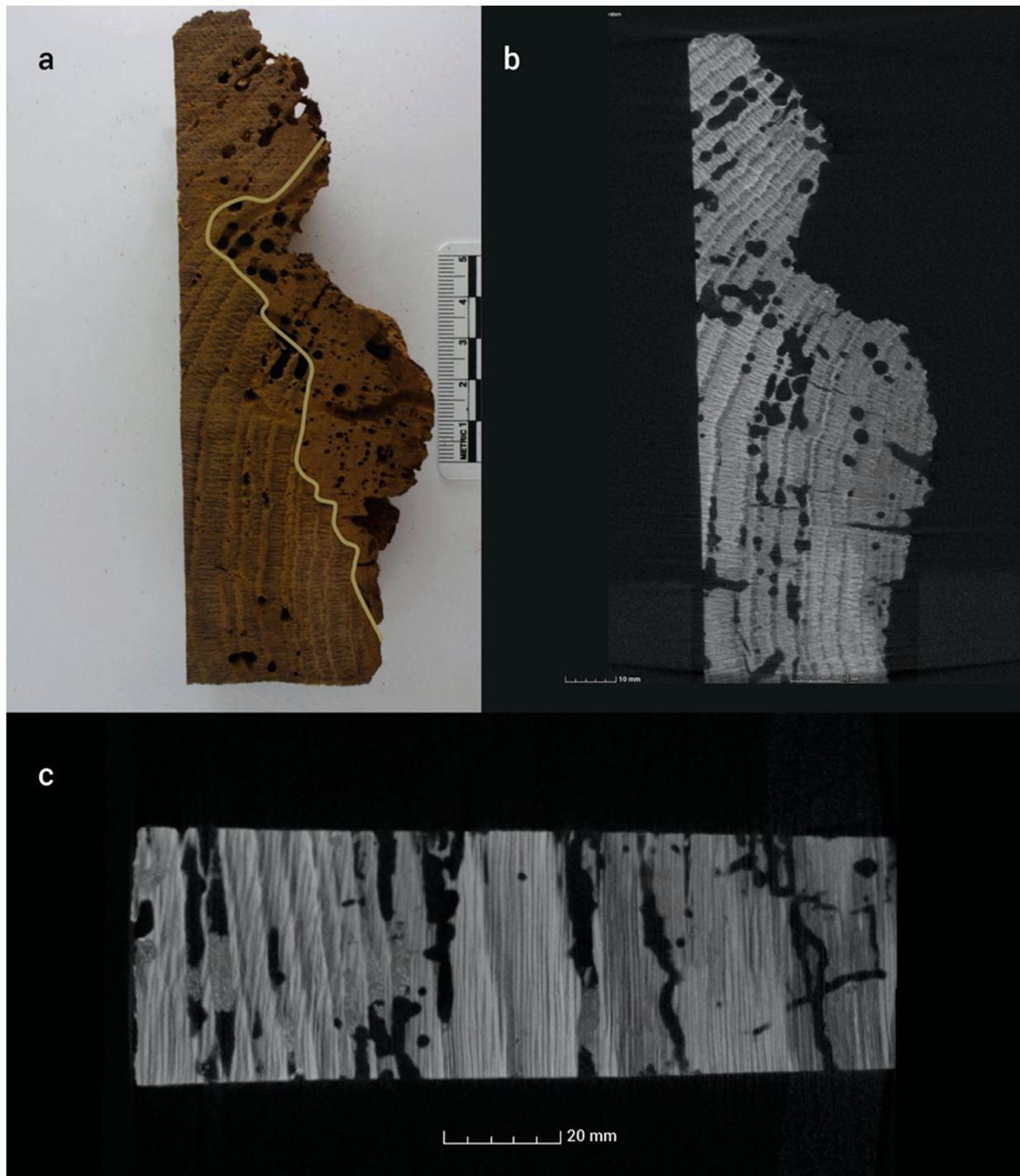The micro-CT slices of Block 1b in Figure 6(b,c) also clearly show extensive internal damage in both

Figure 6. Images of Block 1b (surface photograph and CT slices). In Figure 6(a), the boundary has been drawn on (by eye), distinguishing (i) the area of degrading wood, lacking some structure (here, the right-hand side of the block) from (ii) the better condition, sound wood (here, the left-hand side of the block). Note that Figure 6(b) is a 'slice' from within Block 1b, and hence the holes are not identical to those observed in the surface image.

the longitudinal and transverse planes. The tunnels are mostly empty of frass and most commonly occurring in the earlywood (visible in *Quercus* by the ring porous large vessels), indicating a dietary preference for this part of the growth ring; reason(s) for which are outlined later.

Block 6a

This is a complete, rectangular block (Figure 7) with a single flight hole on the original outer edge (Figure 7 (d)) and less extensive internal damage (Figure 8).

The micro-CT slices from Block 6a suggest a tendency for the avoidance of particularly large multiseriate rays (Figure 8(a)) and show a preference for the longitudinal alignments of the tunnels (Figure 8(b, c)). Figure 8(b) also shows a characteristic right-angle turn of the tunnel. Frass is observed within some of the tunnels, in particular in Figure 8(c).

Isolating and inverting the tunnel volumes from the wood matrix helps to visualise their form (e.g. Figure 9), particularly the prevalence of longitudinally-aligned linear tunnels. It should be noted that some tunnels are 'lost' during this process or appear as patches of noise on the images due to the difficulty in digitally isolating the frass from the wood matrix (see further discussion, below).

Block 7a

Although this is not a complete rectangular block (Figure 10), some area of its original outer edge (Figure 10(b)) still remains, on which there is a single flight hole.

The micro-CT slice of this block (Figure 11(b)) shows a distinct change in direction of a tunnel. It gets very close (<1 mm) to the (original, darkened) outermost edge of the timber, but then turns away, inwards. From there, it seems to follow a crack (i.e. a pre-existing weakness) in the wood and continue in a direction oblique to (i.e. cross-cutting) radial structures, before reaching a region of extensive damage. Other tunnels are within the earlywood of a growth ring (Figure 11(b)). Some tunnels are clearly empty, while others nearby are packed with frass (Figure 11 (c)). Another change in direction can be seen in Figure 11(d).

Quantification of Surface Tunnel Area and Internal Tunnel Volumes

The total area of flight holes on the photographed surfaces of each block are presented in Table 2. Comparison of the calculated area with a visual inspection of the images indicates that while the method can detect flight tunnels on the surface of
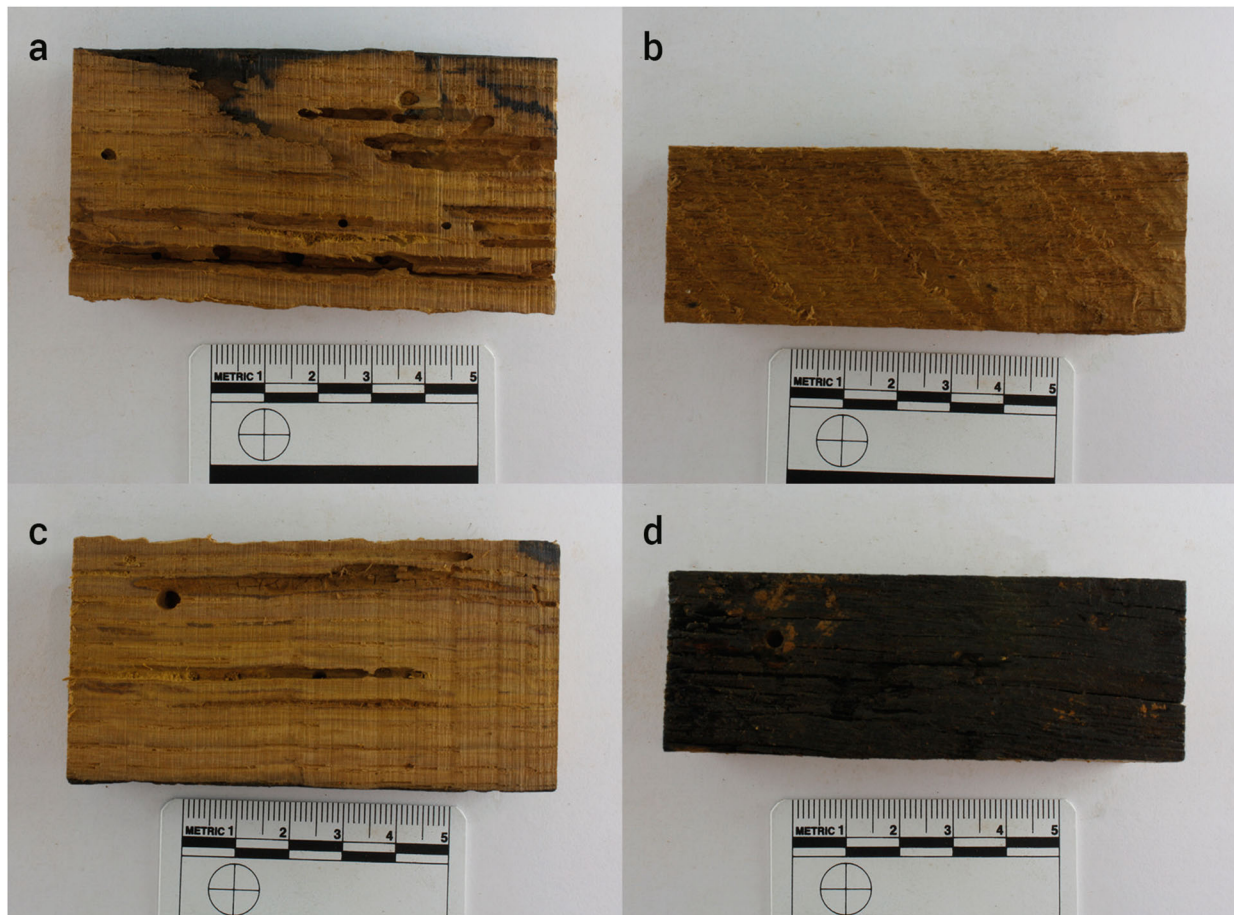

Figure 7. Block 6a, showing the reverse faces on the top and bottom rows.
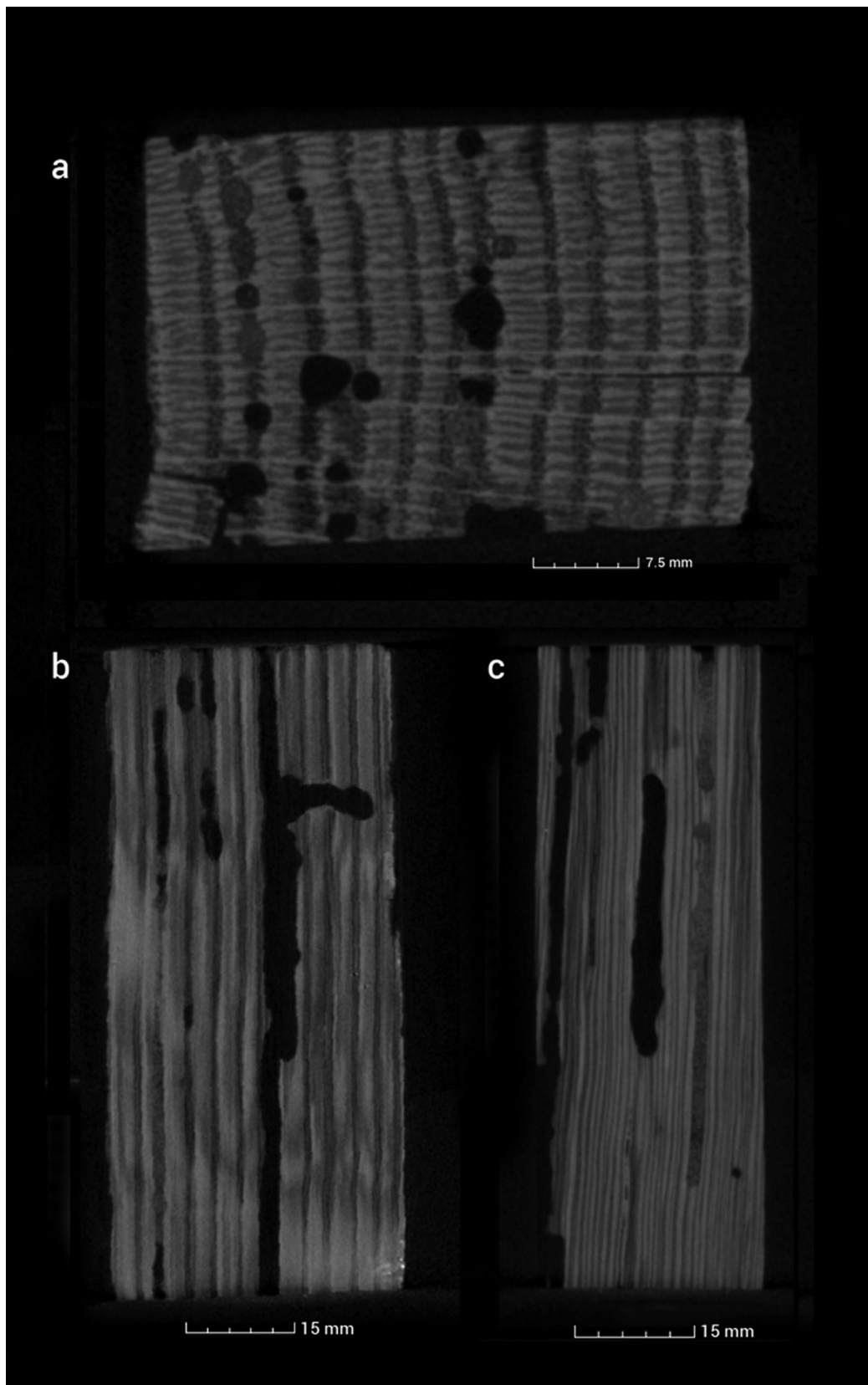
Figure 8. Micro-CT slices from Block 6a: (a) transverse, and (b) and (c) longitudinal.

lighter coloured wood (broken, eroding surfaces), those on the (original) external surfaces of the wood which were darker in colour (e.g. Block 6a, Figure 7(d)) were not always detected due to insufficient contrast between the holes and the wood surface.

Further difficulties were experienced in calculating the total area of flight holes for samples that had significant damage resulting in uneven surfaces (e.g. Block 7a, Figure 10). Unfortunately, these difficulties could not be overcome by calculating the flight hole area from the micro-CT images using the same

Figure 9. Model of the tunnel voids from Block 6a. Total height of block is ca. 90 mm.

process because the uneven surfaces resulted in the uppermost slices being incomplete. Even when the software's register function was applied, it was almost always impossible to get a sufficiently complete image of an individual surface which would ensure that all the true external edges of the flight holes were visible. Analysis of these slices could therefore have excluded entire or partial flight holes that were visible on the photographs, and analysis of deeper slices could have included tunnels that stopped just below the surface (e.g. the tunnel with the abrupt turn in Figure 11 (b)).

Total tunnel volume was calculated twice for each block of wood, using micro-CT image slices in two different planes perpendicular to each other. For all blocks, the two volumes were in good agreement with each other and the mean values are presented in Table 2. However, quantifying the data was challenging and volumes must be assumed to be a 'best estimate' rather than an accurate measurement. The tunnel volume was calculated by setting voxel

greyscale threshold boundaries to discriminate between the empty tunnels and the surrounding wood. However, cracks and other natural variations within the wood such as knots may have been included in the lower greyscale ('black') segment as their voxel density was indistinguishable from the empty tunnels, which may have resulted in artificially high tunnel 'volume' measurements. Conversely, the voxel greyscale density of the frass in some, but not all, of the galleries was almost identical to that of the surrounding wood, in particular the early wood, making it virtually impossible to distinguish between the two materials and likely resulting in underestimating the total tunnel volume measurements.

Calculating the tunnel volume using VG Studio-Max data also resulted in similar values for intact blocks but encountered the same challenges in discriminating between frass and wood, and cracks and empty tunnels. However, the method applied was affected more strongly by the loss of total sample area analysed (in particular when cropping and removing air from incomplete, irregular-shaped blocks) than the method applied using ImageJ, potentially resulting in a greater reduction of the total sample area analysed.

Despite the difficulties described in measuring both the area of exit holes on the surface of, and the volume of tunnels within, each block, there appears to be a general correlation between the two values (Figure 12), indicating that the number of exit holes may be able to inform on the extent of internal damage.

Discussion

Observing Beetle Activity

The micro-CT images provide valuable information about the insects' activity, in particular the differences in tunnelling behaviour between adult and larval forms of the deathwatch beetle. To the authors' knowledge, this is the first work modelling deathwatch beetle activity in such detail.

Larvae generally tunnel along the grain (i.e. longitudinally through the timber) removing the cells laid down early in the growth season (early-wood) which is higher in nitrogen. The longitudinal configuration is shown well in Block 6a (Figure 8(b,c), and Figure 9), and the preference for the early-wood is best shown in Blocks 1b (Figure 6) and 7a (Figure 11(a, b)). In Block 6a (Figure 8(a)), the tendency for the insects to avoid the widest multiseriate rays is thought to be because of the physiology of the rays themselves, which are harder for the insects' mandibles to cut through.

Once the larva has sufficient energy reserves, it creates a pupal chamber where it pupates into an

Figure 10. Block 7a (image of the fourth surface not available).

adult insect. On emergence, the adult needs to leave the timber as quickly as possible before it depletes its fixed energy store, and, unable to turn round in the confined space, will start tunnelling in the direction it is facing. Because the insects can also determine which way is out, after pupation adults may then need to change the course they were facing. To do this in living, standing trees, the adults will either be following a chemical gradient of increasing nitrogen from heartwood to sapwood or using
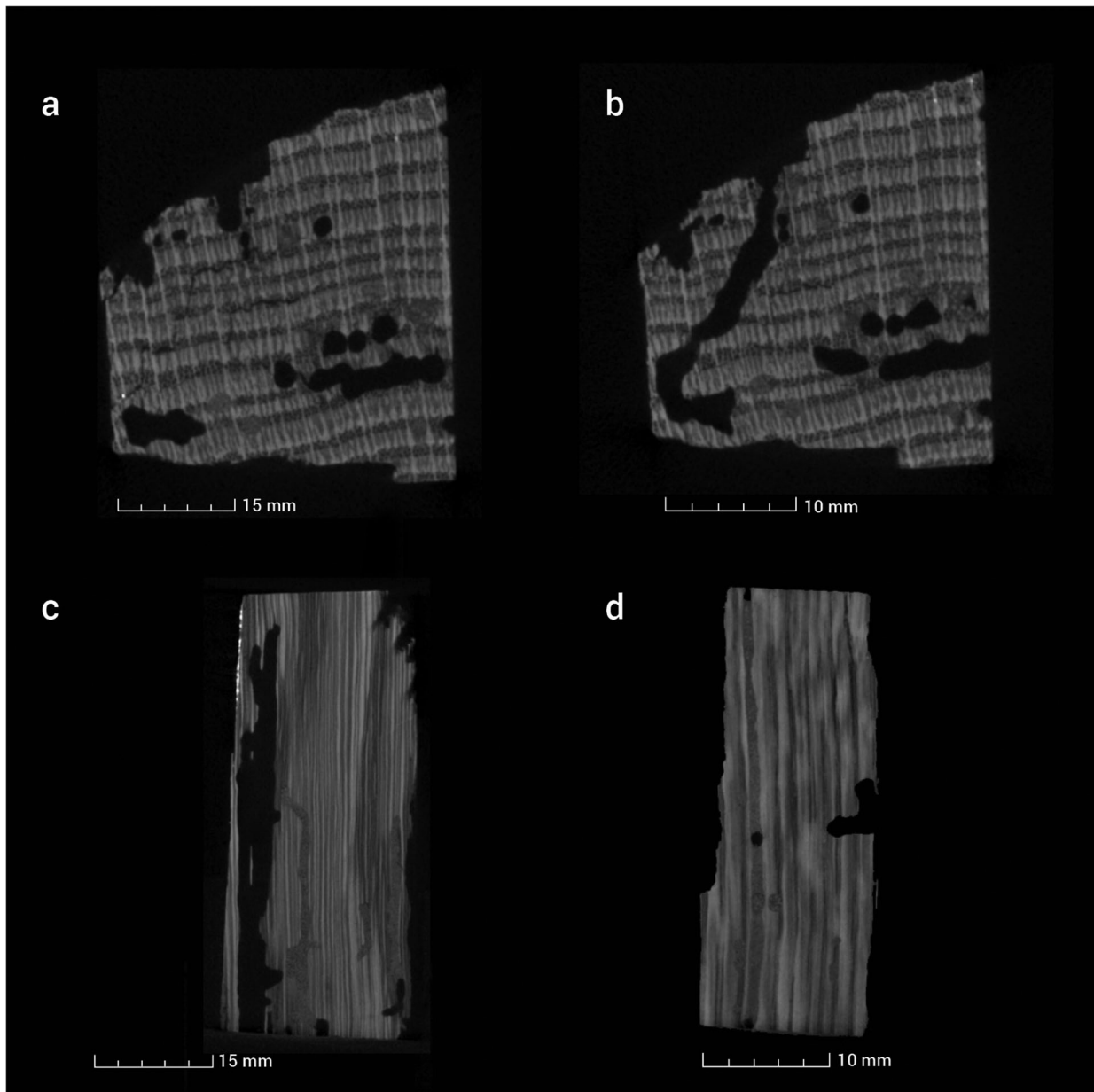
Figure 11. Micro-CT slices of Block 7a: transverse (a and b) and longitudinal (c and d).

vibration sensation to work out where the surface is relative to itself.

This reorientation towards the surface can produce abrupt changes in the direction of a tunnel, as seen in Block 6a (Figure 8(b)) and Block 7a (Figure 11(b,d)). This tunnelling behaviour is different to that of the larvae; most notably that the adults now chew across the grain to get out. It is interesting to note that in Block 7a, the tunnel gets very close to what is thought to be the real original outer face of the timber (the smooth, dark-coloured surface).

Within Block 1b, the tunnels are observed to be of different diameters, but rather than represent damage from other (smaller) taxa, they are thought to all result from deathwatch beetle; the quality of the wood affects insect sizes, and this is what is thought to be reflected here, with changing timber condition over time.

When zooming in as far as possible to the voxel limit on the isolated tunnel volumes (Figure 9) using the VG StudioMax software, a semi-regular, characteristic pattern appears to be visible along the length of the tunnels. Images are not presented here as the resolution is not sufficiently high to provide confidence that these are an actual feature, rather than an artefact of imaging. However, such patterns should not be unexpected, due to the tunnelling physics of the larval stage of wood-boring insects, which exert hydrostatic pressure against the walls with the front end of their bodies to get purchase on the face of the tunnel. Once the larva has eaten all the timber within reach, it deflates, shuffles forward, inflates at a tunnel face, and begins again. Such activity can only be seen using X-radiographic techniques, as once a tunnel is sectioned open, it loses pressure. Micro-CT-scanning smaller

Table 2. Total surface area of flight holes and mean tunnel volume are given for each wood block.

Sample	Total surface area of flight holes (mm^2)	% of surface with flight holes	Mean tunnel volume (mm^3)	% volume of tunnels
1a	763.3	2.1	4208.7	0.88
1b	1343.9	4.1	15938.4	4.15
2a	108.7	–	8615.6	–
2b	120.1	0.8	7532.6	3.67
3a	0	0	0	0
3b	722.3	2.2	8441.4	2.13
4a	0	0	0	0
4b	1070.6	3.2	5652.6	1.40
5a	2955.0	9.2	28415.0	6.73
5b	2023.8	9.8	22095.3	6.38
6a	229.1	1.5	6792.3	4.71
6b	78.7	0.4	2545.4	0.99
7a	215.1	1.2	9564.1	4.62
8a	142.5	0.7	2965.4	1.34
8b	135.1	0.7	3064.7	1.28

Notes: The percentage of the total surface area comprised of exit holes, and the total volume of each block that is estimated to be comprised of tunnels is also given (except for Block 2a which was an irregular prism-shape and the volume could not accurately be calculated). The total surface area is calculated from the four surfaces that were photographed and analysed for exit holes and not the total surface area of each block.

blocks of wood, at higher resolutions than used within this initial study, may reveal evidence of this activity.

External Damage

Although the flight holes on the original outer timber faces could be spotted visually by eye, the image analysis software was sometimes unable to differentiate them from the dark colour of the surrounding exposed wood; the pixel intensity was often too similar for both the darker wood and the flight holes to be separated, even with various adjustments to the image settings. The image analysis was also problematic for blocks with uneven surfaces where the wood was broken and disintegrating.

The use of extreme acute angle lighting (rather than diffused lighting) may improve the image quality and the potential to differentiate dark holes from dark wood on relatively even surfaces using this approach, but may not be sufficient on uneven surfaces. It may be possible to digitally improve the images individually as required or to manually isolate each flight hole by digitally drawing a circle around it and treating each hole as an individual object rather than trying to determine all holes on a particular surface at once. However, both these approaches would be time-consuming and introduce the potential for human error into the calculation of flight hole area.

This method was most successful on the smooth surfaces that had been produced by sawing during sub-sampling of the timbers, which would be unlikely to be available if studying *in-situ* timbers or historical artefacts. Unfortunately, this study has demonstrated that this digital technique would not be suitable for accurately identifying and quantifying insect damage on existing photographs, for example, those taken on-site of *in-situ* timbers.
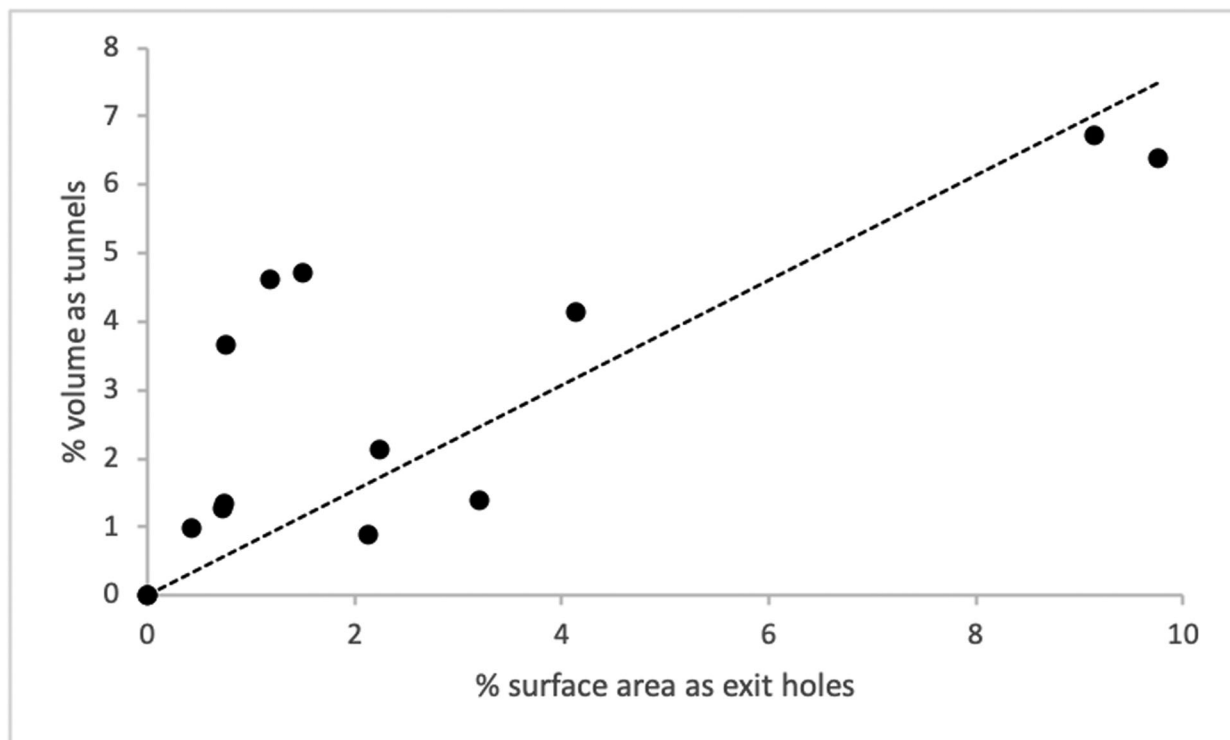

Figure 12. Plot showing % surface area as exit holes vs % total block volume as tunnels, showing broad correlation between the two measurements. The trendline is forced to pass through 0 on both axes to reflect expected values for unaffected wood.

Quantifying Internal Damage

The micro-CT scans of the wood successfully show the internal damage caused by insect infestation; it is possible to visually differentiate the tunnels from the surrounding wood, even when the tunnels are frass-filled.

Unfortunately, as densely packed frass (present in many galleries in these samples) has a very similar pixel greyscale intensity to the surrounding wood, it was not possible to accurately calculate the overall tunnel volume of each block. While this approach has been applied successfully for marine bivalve tunnels in wood (Amon et al. 2015; Amon et al. 2016), the bivalves leave the tunnel empty with the exception of calcium carbonate shells and linings, which have a distinctly different pixel intensity to both the wood and the empty tunnels, allowing a third segment to be created and extracted from the total sample volume. While micro-CT scanning of smaller blocks of wood – allowing for higher magnification and spatial resolution – may enhance the digital separation of the frass from the surrounding wood matrix (especially with the application of double thresholding (e.g. Steppe *et al.*, 2004)), this requires a compromise with a smaller, and potentially less representative, volume being interrogated and would not overcome the challenge of digitally separating knots and cracks from empty tunnels.

Despite the difficulties in calculating the flight hole area and tunnel volumes as already discussed, there appears to be a broad correlation between the total area of flight holes on the surface of the blocks and the internal tunnel volume (Figure 12). However, this correlation must be interpreted with caution for several reasons. Differences in the rate of growth and quality of the timber, and its environmental fate over the larval phase of the beetles' lifespan (five years or more, on average) make confident interpretation of the data challenging. Additionally, the blocks were not photographed in the same orientation, and images were only taken of four faces. Due to sub-sampling of the large timber, only some of the surfaces analysed were, therefore, external surfaces of the overall timber, with true 'flight' holes; many of the holes recorded on the other surfaces simply indicate movement of the beetles within the timber itself, or into adjacent timbers. This approach may be suitable for smaller wooden objects such as print blocks (e.g. Hedges 2012), but not for *in situ* timbers, or larger ones that cannot be sub-sectioned for micro-CT scanning.

Research and Application Potentials

The results of this pilot study have successfully demonstrated the role of micro-CT scanning in revealing aspects of the tunnelling habits of wood-boring insects – here, deathwatch beetle – which take place hidden from view. This technique could similarly be applied to damage from other wood-boring insects.

As discussed here, both micro-CT scanning and X-radiography have also differentiated between good and poor condition wood resulting from reasons other than wood-boring infestations; this indicates the potential capability of identifying wood degraded by other causes. Mechanisms responsible for such 'softening' can include wood rot or chemical damage from cleaning and treatments. Although not much is known about the history of the specific timber studied after its removal from *Victory*, it is understood that when it was *in situ* it was beyond reach of any direct treatment. Therefore, if the deterioration is due to rot, then the white rot decay mechanism is a likely candidate given the genus, age and quality of the timber; in fact, white rot has been recorded more-recently during routine survey elsewhere on the ship (Downes 2016; also see Davis, 2020). Further research would be needed to establish how such damage (from confirmed rot identification(s)) can be detected using X-radiographic imaging techniques.

During the course of this study, compression testing was carried out on the samples in order to investigate the structural integrity of the wood blocks, by determining the force required to compress a block of wood by 2 mm (Southwell 2017). As would be expected, the results appeared to correlate with internal tunnel volume; the higher the total internal tunnel volume, the less force required to compress the sample. The data are not included here due to unresolved uncertainties in recording the samples' identifiers and whether all the samples were processed with the wood grain in the same orientation. In addition, the degree of microbial/fungal decay in the timber prior to deathwatch beetle infestation is unknown; such decay factors will affect the integrity of the wood, yet are unquantified. Despite this, if the study was to be continued, exploring the role of compression testing further as a tool to investigate at what point the volume of tunnels begins to affect an historical timber's structural integrity, is considered of value. Carrying out such tests on a smaller, micron scale is also recommended, in order to assess the effect of the preferential removal of the early wood by the deathwatch beetle.

Conclusions

This work has successfully demonstrated the use of micro-CT scanning in the study of wood-boring insects within wood. In particular, it has allowed the visualisation of deathwatch beetle activity within a historic timber. However, it required sub-sampling the timbers to get suitably-sized samples that will fit in the micro-CT scanner (here, the maximum size was 12 cm in height).

As well as the insect damage, the work has also identified internal differences in wood condition thought to result from rot, demonstrating the potential for the application of the technique beyond the original research questions. This has implications for the study of the symbiotic relationship between the insects themselves and fungal degradation.

The study has identified two main challenges for the quantification of beetle damage to wood using digital techniques. Firstly, the difficulty in quantifying the area of flight holes on darkened and/or uneven surfaces. Secondly, the difficulty in quantifying the tunnel volume due to the similarity in pixel density of the wood matrix and frass-filled tunnels makes it very hard to digitally separate the two materials. (This similarity is unsurprising given that wood dust comprises a significant proportion of frass). This is in contrast with studies of other wood borers which leave their tunnels empty, or with a calcareous lining which is of a significantly different pixel intensity to both the wood and the empty tunnels.

Nonetheless, this work has successfully begun a train of research directly relevant to heritage conservation, and thus with real-world applications; the threat of degradation to historic materials caused by wood-boring insects is constant and relentless (see Davis, 2020). Further work is required to confirm the correlation between surface exit holes and internal damage. Given that the current management plan for *Victory* clearly states a preference for preservation of timbers *in-situ* and the avoidance of unnecessary removal of historic fabric, understanding the degree and extent of such damage is even more crucial. If the correlation can be demonstrated with confidence then the analysis of surface flight holes from digital images of the external surfaces of timbers may be incorporated into future conservation management of *Victory*.

Acknowledgements

Disclosure Statement

No potential conflict of interest was reported by the authors.

Notes on contributors

Fiona Brock is Lecturer in Applied Analytical Techniques at Cranfield University's Forensic Institute. With a degree in chemistry, her original research interests were in biogeochemistry, before joining the radiocarbon laboratory at Oxford University. Since then, she has gained extensive experience of applying analytical techniques to archaeological science research, working on materials including bone, wood, charcoal and parchment, in particular from the UK and the Caribbean.

Richard Southwell holds the position of Failure Analysis Engineer (Photonic Devices), responsible for material characterisation and defect analysis in an R&D environment currently transitioning to industrial scalability. He previously studied Forensic Engineering & Science at Cranfield University. This work formed part of his MSc research dissertation to determine whether micro-CT was a suitable tool to image deathwatch beetle infestation of historic maritime timber.

Zoë Hazell is Senior Palaeoecologist at Historic England. She has a Geography (Quaternary Science) background, with research experience in the reconstruction of past environments and landscapes. Her multidisciplinary interests mean that she has worked on diverse projects, from the use of peatlands to reconstruct past climatic conditions to the study of wood use through the identification and recording of waterlogged wood and wood charcoal remains from archaeological sites.

Roland Wessling is a lecturer in Forensic Archaeology and Anthropology at Cranfield University's Forensic Institute. While his fieldwork consists mostly of mass grave instigations, recovery of conflict causalities and geophysics, Roland's research centres around the creation and interrogation of images and 3D models of both objects, such as bones, toolmarks or historic artefacts, and incident scenes, including grave sites, crime scenes and wider forensic landscapes.

Matthew Green studied Biology and Applied Entomology before undertaking a PhD studying the ecology of a wood-boring weevil introduced to the UK from New Zealand. He has over 15 years' experience in timber condition surveying and building pathology alongside urban insect pest control and building hygiene. Splitting his time between timber bio-deterioration and urban pest control, he manages a pest insect laboratory and undertakes commercial research into urban insect pest control. He lectures on water movement in buildings and timber decay in his spare time.

Diana Davis holds the current position of Head of Conservation at the National Museum of the Royal Navy, responsible for preventive and interventive conservation of the historic fabric of, and objects within, the museum's collection of historic ships and submarines. She has previously worked as a conservator for National Museums Scotland, the Science Museum and English Heritage, and prior to this her background was in archaeology.

ORCID

Fiona Brock http://orcid.org/0000-0003-0728-6091

References

Amon, D. J., D. Sykes, F. Ahmed, J. T. Copley, K. M. Kemp, P. A. Tyler, C. M. Young, and A. G. Glover. 2015. "Burrow Forms, Growth Rates and Feeding Rates of

Wood-Boring Xylophagaidae Bivalves Revealed by Micro-Computed Tomography." *Frontiers in Marine Science* 2: 10. doi:10.3389/fmars.2015.00010.

Bird, M. I., P. L. Ascough, I. M. Young, C. V. Wood, and A. C. Scott. 2008. "X-Ray Microtomographic Imaging of Charcoal." *Journal of Archaeological Science* 35: 2698–2706. doi:10.1016/j.jas.2008.04.018.

Brodersen, C. R. 2013. "Visualising Wood Anatomy in Three Dimensions with High-Resolution X-Ray Micro-Tomography (μCT): A Review." *IAWA Journal* 34 (4): 408–424. doi:10.1163/22941932-00000033.

Bugler, A. 1966. *HMS Victory: Building, Restoration and Repair*. London: HMSO.

Davis, D. 2018. *HMS Victory: Integrated Pest Management Strategy September 2018*. NRMN internal report.

Davis, D. 2020. "Wood-Borers in Historic Ships." *Environmental Archaeology*. (This volume).

Downes, S. 2016. *HMS Victory: Results from Sampling for Fungal Contamination*. Personal communication for NMRN (unpublished).

Eriksen, A. M., D. J. Gregory, C. Villa, N. Lynnerup, K. B. Botfeldt, and A. R. Rasmussen. 2016. "The Effects of Wood Anisotropy on the Mode of Attack by the Woodborer *Teredo navalis* and the Implications for Underwater Cultural Heritage." *International Biodeterioration & Biodegradation* 107: 117–122. doi:10.1016/j.ibiod.2015.11.1018.

Haneca, K., K. Deforce, M. N. Boone, D. Van Loo, M. Dierick, J. Van Acker, and J. Van Den Bulcke. 2012. "X-Ray Sub-Micron Tomography as a Tool for the Study of Archaeological Wood Preserved Through the Corrosion of Metal Objects." *Archaeometry* 54 (5): 893–905. doi:10.1111/j/1475_4754.2011.00640.x.

Hedges, S. B. 2012. "Wormholes Record Species History in Space and Time." *Biology Letters* 9: 20120926. doi:10.1098/rsbl.2012.0926.

Hickin, N., and R. Edwards. 1975. *The Insect Factor in Wood Decay: An Account of Wood-Boring Insects with Particular Reference to Timber Indoors*. 3rd (revised) ed. New York: St. Martin's Press.

Jennings, J. T., and A. D. Austin. 2011. "Novel Use of a Micro-Computed Tomography Scanner to Trace Larvae of Wood Boring Insects." *Australian Journal of Entomology* 50: 160–163.

Knight, K. Y., T. A. Cousins, and D. Parham. 2019. "A Comparison of Biodegradation Caused by Teredinidae (Mollusca: Bivalvia), Limnoriidae (Crustacea: Isopoda), and *C. terebans* (Crustacea: Amphipoda) Across 4 Shipwreck Sites in the English Channel." *J. Archaeological Science: Reports* 23: 854–867. doi:10.1016/j.jasrep.2018.12.005.

Lehmann, P., M. Javal, A. Du Plessis, and J. S. Terblanche. 2021. "Using μCT in Live Larvae of a Large Wood-Boring Beetle to Study Tracheal Oxygen Supply During Development." *Journal of Insect Physiology* 130: 104199. doi:10.1016/j.jinsphys.2021.104199.

McCaig, I., and B. Ridout 2012. *Practical Building Conservation: Timber*. English Heritage. Farnham: Ashgate Publishing Limited.

McGovern, M., A. Senalik, G. Chen, F. C. Beall, and H. Reis. 2010. "Detection and Assessment of Wood Decay Using X-ray Computer Tomography." Proc. SPIE 7647, Sensors and Smart Structures Technologies for Civil, Mechanical and Aerospace Systems 2010. doi:10.1117/12.843709

McGowan, A. 1999. *HMS Victory: Her Construction, Career and Restoration*. London: Chatham Publishing.

Schindelin, J., I. Arganda-Carreras, E. Frise, V. Kaynig, M. Longair, T. Pietzsch, S. Preibisch, et al. 2012. "Fiji: An Open-Source Platform for Biological-Image Analysis." *Nature Methods* 9: 676–682. doi:10.1038/nmeth.2019.

Schweingruber, F. 1990. *Microscopic Wood Anatomy: Structural Variability of Stems and Twigs in Recent and Subfossil Woods from Central Europe*. 3rd ed. Birmensdorf: Swiss Federal Institute for Forest, Snow and Landscape Research.

Southwell, R. J. 2017. "An Investigation into the Structural Integrity of Oak Beam Timber Exposed to Invasive *Xestobium rufovillosum* from HMS Victory Utilizing Micro-CT and Other Methods." MSc thesis, Cranfield University.

Stelzner, J., and S. Million. 2015. "X-Ray Computed Tomography for the Anatomical and Dendrochronological Analysis of Archaeological Wood." *Journal of Archaeological Science* 55: 188–196. doi:10.1016/j.jas.204.12.015.

Steppe, K., V. Cnudde, C. Girard, R. Lemeur, J.-P. Cnudde, and P. Jacobs. 2004. "Use of X-ray Computed Microtomography for Non-Invasive Determination of Wood Anatomical Characteristics." *Journal of Structural Biology* 148 (1): 11–21. doi:10.1016/j.jsb.2004.05.001.

Ungurean, B. 2012. "The Conservation of Wooden Heritage Items Exhibited in the Open Against the Attack of Noxious Insects." *Academy of Romanian Scientists Annals Series on Biological Sciences* 1 (2): 6–31.

Van den Bulcke, J., M. Boone, J. van Acker, M. Stevens, and L. van Hoorebeke. 2009. "X-Ray Tomography as a Tool for Detailed Anatomical Analysis." *Annals of Forest Science* 66: 508–519. doi:10.1051/forest/2009033.

Van den Bulcke, J., B. Masschaele, M. Dierick, J. van Acker, M. Stevens, and L. van Hoorebeke. 2008. "Three-Dimensional Imagining and Analysis of Infested Coated Wood with X-Ray Submicron CT." *International Biodeterioration & Biodegradation* 61: 278–286. doi:10.1016/j.iniod.2007.09.004.

Whitau, R., I. E. Dilkes-Hall, E. Dotte-Sarout, M. C. Langley, J. Balme, and S. O'Connor. 2016. "X-ray Computed Microtomography and the Identification of Wood Taxa Selected for Archaeological Artefact Manufacture: Rare Examples from Australian Contexts." *Journal of Archaeological Science: Reports* 6: 536–546. doi:10.1016/j.jasrep.2016.03.021.